INFRARED SPECTROPHOTOMETRY OF THREE SEYFERT GALAXIES AND 3C 273

R. M. CUTRI,[1] D. K. AITKEN,[2,3] B. JONES,[1,4] K. M. MERRILL,[4]
R. C. PUETTER,[1] P. F. ROCHE,[3] R. J. RUDY,[1] R. W. RUSSELL,[1,5]
B. T. SOIFER,[1,6] AND S. P. WILLNER[1]

ABSTRACT

Spectrophotometry from 2.1 to 4.0 μm of the Seyfert galaxies NGC 1068, NGC 4151, and Mrk 231 and of the QSO 3C 273 is presented, along with some observations of NGC 4151, Mrk 231, and NGC 1068 at longer wavelengths. The spectrum of NGC 1068 is found to consist of a stellar component and a component which declines steeply toward shorter wavelengths below 4 μm. The previously observed 12.8 μm [Ne II] emission line is not confirmed. Infrared variability in NGC 4151 is confirmed. The simplest model for its energy distribution consists of three components, all having constant spectral shapes and only one component being variable. A dip in the spectrum at 10 μm is confirmed in Mrk 231, but no narrow structure was seen in the region of the possible 3.5 μm emission reported by Rieke. Some structure may have been detected between rest wavelengths of 2.8 and 2.9 μm in Mrk 231, and the spectrum is not an exact power law. The spectrum of 3C 273 beyond 3 μm is consistent with a power law, although some structure might be present, and there are deviations from the power law at shorter wavelengths.

Subject headings: galaxies: Seyfert — infrared: sources — infrared: spectra — quasars

I. INTRODUCTION

The galaxies NGC 1068, NGC 4151, and Markarian (Mrk) 231 are among the most comprehensively studied Seyferts in the infrared. 3C 273 is similarly well documented for a QSO. Ever since the infrared excess in NGC 1068 was first observed by Pacholczyk and Wisniewski (1967), several surveys, such as those of Rieke and Low (1972), Penston *et al.* (1974), Allen (1976), Rieke (1978), and McAlary, McLaren, and Crabtree (1979), have included photometric coverage of these objects. Theoretical analysis of the infrared radiation from these galaxies has been included in discussions by Burbidge and Stein (1970), Jones and Stein (1975), Stein and Weedman (1976), and Jones *et al.* (1977).

Prominent among the questions still being pursued is whether the infrared spectra of Seyfert galaxies can be generally characterized by a single power law presumably arising from a nonthermal source, or whether a composite of several spectral components, originating from different sources within the nuclei, is required (see e.g., Rieke and Lebofsky 1979). Working from the extensive prelude of photometric and theoretical information, more detailed spectrophotometric studies are the next logical step to take in approaching some of the remaining questions. Four such works already available have found:

silicate absorption in NGC 1068 (Kleinmann, Gillett, and Wright 1976); molecular hydrogen, He I, and Bγ emission also in NGC 1068 (Thompson, Lebofsky, and Rieke 1978); and the identification of Pα in 3C 273 (Grasdalen 1976; Puetter *et al.* 1978).

This paper presents 2–4 μm spectrophotometry of the Seyfert galaxies NGC 1068, NGC 4151, Mrk 231, and of the QSO 3C 273. In addition, 8–13 μm broad-band measurements were obtained for NGC 4151 and Mrk 231, as well as some 8–13 μm narrow-band measurements for Mrk 231 and a new 8–13 μm spectrum of NGC 1068. In the first two objects, the emission contains a significant component due to stars, especially at the shorter wavelengths. Subtracting this component from the spectrum of NGC 1068 reveals that the remaining spectral distribution, due to the central source, falls off rapidly toward shorter wavelengths. This is consistent with other observations that have suggested that the origin of the excess infrared radiation beyond 5 μm is mostly thermal reradiation by dust. These previous studies of NGC 1068 include the measurement of finite angular size at 10 μm (Becklin *et al.* 1973), and the presence of silicate absorption at 10 μm and emission at 20 μm (Rieke and Low 1975; Kleinmann, Gillett, and Wright 1976; Lebofsky, Rieke, and Kemp 1978). Polarimetric observations between 0.35 and 3.5 μm (Angel *et al.* 1976; Lebofsky, Rieke, and Kemp 1978) have shown a complex polarization structure in the nucleus, and a contribution by nonthermal radiation is probably also required.

Broad-band observations from 2 to 4 μm obtained in the course of this study confirm the variability of NGC 4151 (Penston *et al.* 1971, 1974; Stein, Gillett, and Merrill

[1] Center for Astrophysics and Space Sciences, University of California, San Diego.
[2] Anglo-Australian Observatory.
[3] University College, London.
[4] School of Physics and Astronomy, University of Minnesota.
[5] Center for Radiophysics and Space Research, Cornell University.
[6] California Institute of Technology.

1974; Lebofsky and Rieke 1980) but show no variability in NGC 1068. This would seem to indicate that there is a nonthermal infrared source in NGC 4151. The shape of the spectrum and magnitude of the variations suggest, however, that there are two components of the flux in addition to starlight: one which is nonthermal and variable contributes significantly at the shorter wavelengths; a second which is relatively constant and probably thermal in origin dominates the flux past 3 μm.

Markarian 231 and 3C 273 show no discernible stellar component, were not seen to vary above the 10% level, and have spectra that approximate power laws. Evidence for a broad minimum in the 8 to 13 μm spectrum of Mrk 231, as reported by Rieke (1976), was found, but insufficient signal-to-noise prevents confirmation of the shape and depth of the feature.

II. OBSERVATIONS

All of the new observations were made with the 1.5 m University of California, San Diego (UCSD)/University of Minnesota telescope at Mount Lemmon, except the 8–13 μm NGC 1068 spectrum and the 6.5 μm broadband measurement of NGC 4151. The 2–4 μm measurements were taken with an InSb photovoltaic detector, with the exception of the 1978 April observation of NGC 4151. This observation, along with all the 8–13 μm photometry, was obtained with a Si:As photoconductor. The 8–13 μm NGC 1068 spectrum was observed with the University College, London dispersing spectrometer, using an array of five Si:As detectors on the Anglo-Australian telescope. Table 1 lists the dates on which each object was observed, along with the portion of the spectrum covered on that date. Broad-band measurements were also obtained on most nights. The beam diameter was 17″, unless otherwise indicated, and the spectral resolution of the narrow-band points was $\lambda/\Delta\lambda \approx 60$. Figures 1 and 2 show the spectra of each of the objects. The 1.9–2.5 μm portion of the spectrum of 3C 273 was taken from Puetter et al. (1978) and has resolution $\lambda/\Delta\lambda \approx 30$.

For each object, the data were reduced against one of a number of standard stars, observed on the same night at a comparable air mass. The assumed fluxes of these standards were normalized to the flux of α Lyr, which was modeled as a 9700 K blackbody having zero color and a flux of 5.7×10^{-14} W cm^{-2} μm^{-1} at 2.0 μm.

TABLE 1

Narrow-Band Wavelength Coverage (μm)

| Date (UT) (year/month/date)	NGC 1068	NGC 4151	Mrk 231	3C 273
75/3/25	...	...	3.2–3.6	...
75/4/28	...	...	3.2–3.7	...
75/4/29	...	3.2–3.4	3.2–3.5	...
75/5/25	...	2.9–4.1	...	...
75/5/26	...	2.9–4.1	3.0–4.0	...
75/6/17	...	...	3.0–4.1	...
76/2/26	...	...	2.1–2.3	...
76/3/8	...	2.2–2.4	...	...
76/3/13	...	2.1–4.1	2.9–3.8	...
76/3/14	...	...	2.9–4.0	...
76/3/22	...	2.1–3.2	...	...
76/3/26	...	2.1–2.5	...	...
76/4/20	...	2.1–4.0	2.2–4.0	...
76/4/24	...	2.1–4.0	...	...
76/5/7	...	2.1–3.8	...	...
76/6/10[a]	8.0–13.4	...	...	...
76/12/12	...	...	11.24	...
77/1/31	...	...	8.0–12.8	...
77/2/4	...	...	10.8–13.2	...
77/3/15	...	...	...	3.8
77/3/19	...	...	...	2.9–3.8
77/4/6	...	2.8–4.0	2.1–2.5	...
77/4/21	...	10.52	10.9	...
77/5/15	...	...	...	3.0–3.8
77/12/3	...	...	2.1–3.6	...
77/12/4	2.1–3.7	2.1–3.6	...	...
77/12/5	2.1–2.6	2.1–2.3	...	...
77/12/6	2.8–3.7	...	...	3.0–3.1
77/12/17	3.2–4.1	...	...	...
78/2/20	2.1–3.4	2.1–2.3	2.2–2.4	...
78/4/28	...	...	...	1.6–2.5
78/9/27	2.1–2.6	...	...	...
78/12/12	...	...	...	3.0–4.0
79/2/9	...	2.1–2.2	...	...
79/3/4	...	...	2.9–3.3	...

[a] 5″ beam.
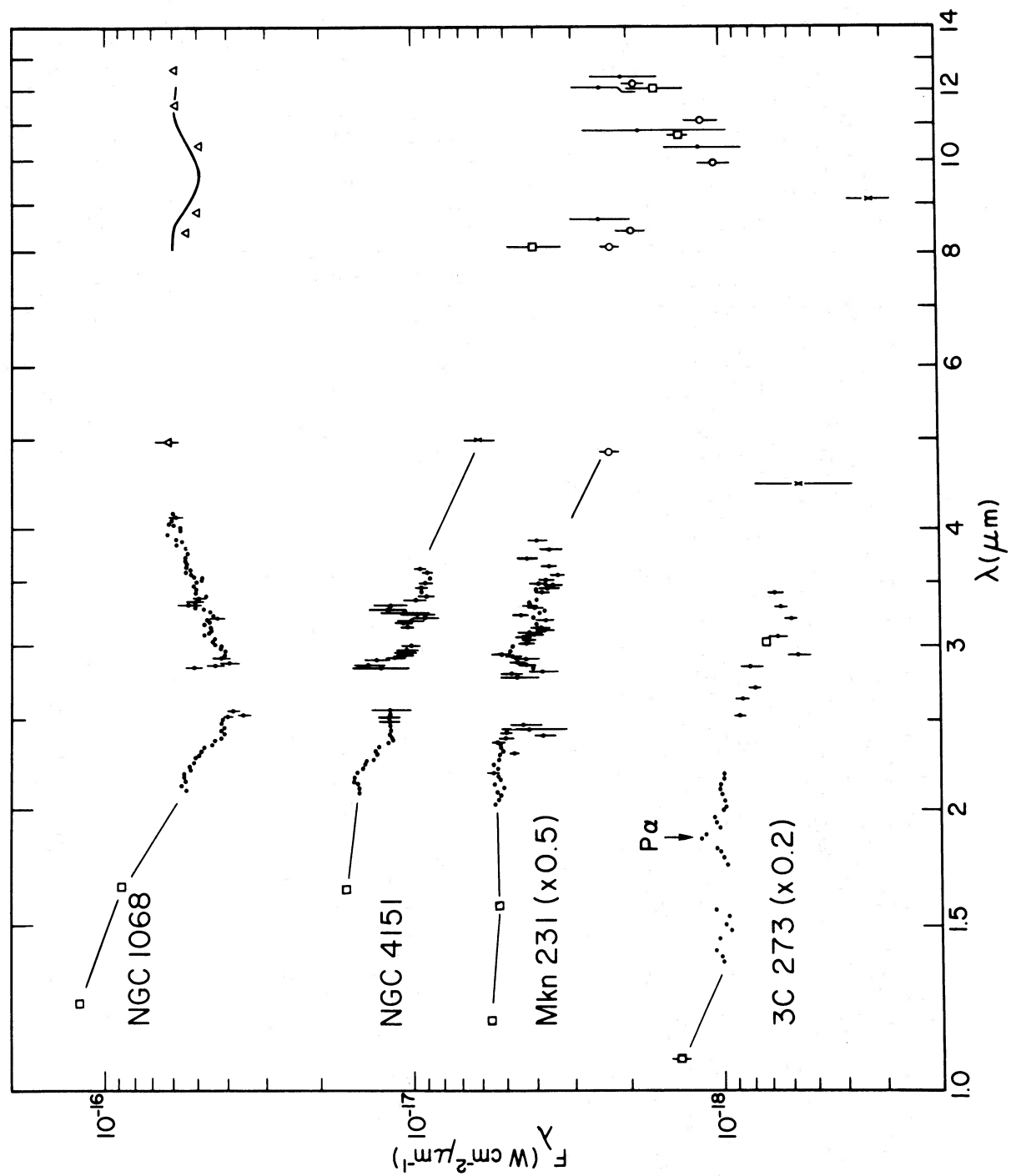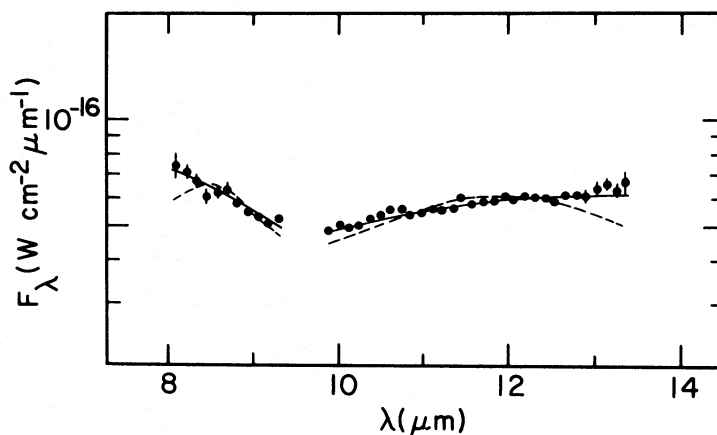
FIG. 2.—The 8–13 μm spectrum and model fits for NGC 1068. The spectral data are represented by the points. The best-fit optically thick model is shown by the solid line, and the best-fit optically thin model is shown by the dashed line (see text).

The data for NGC 1068, Mrk 231, and 3C 273 represent averages of several nights' observations, each night's data being weighted according to the statistical uncertainties. Because of improvements in the detector signal-to-noise in 1977, some of the earlier 2.1–2.5 μm measurements of NGC 1068 that were comparatively noisy were excluded from the average.

As seen in Table 1, not all wavelengths were observed on all nights. If individual data sets differ in overall level, averaging nights with incomplete wavelength coverage can produce spurious features. The spectra for different nights were normalized according to the broad-band measurements, but the existence of spurious features cannot entirely be excluded. The apparent structure between 2.8 and 2.9 μm in Mrk 231, discussed below, may be an example of such a feature.

The data for NGC 4151 were also reduced against various standard stars, η UMa and α Leo being used most frequently. There were observations at both maximum and minimum, using the same standard stars, and no correlation between the galaxy's brightness and the standard star used was observed. We conclude, then, that the variations in the flux level of NGC 4151 are real and not a systematic effect. Light curves of NGC 4151 over the time scale of our observations are shown in Figure 3, and Table 2 lists the broad-band measurements and the dates on which they were obtained. The uncertainties in the measurements are ~ 0.05 mag unless otherwise indicated.

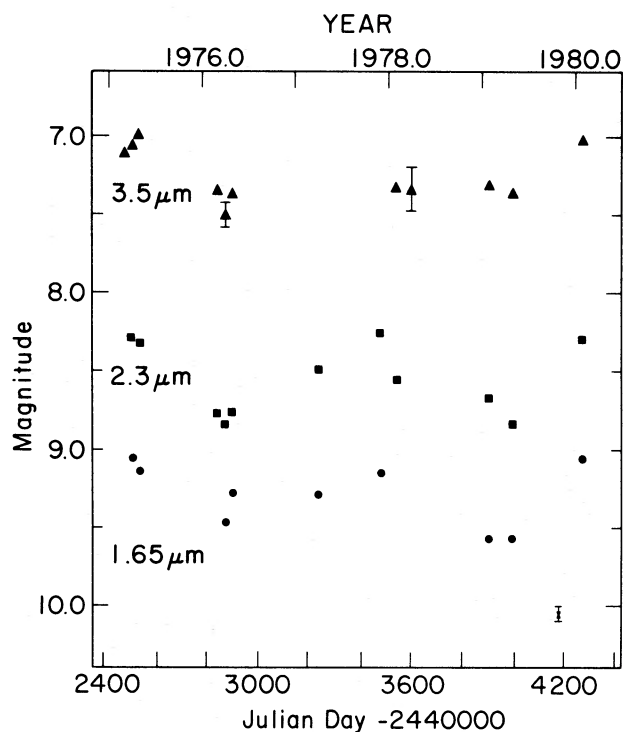Because of the variation in the flux level of NGC 4151, a simple average of the data would be misleading. Our

FIG. 3.—Light curves of NGC 4151 at 1.65 μm (*points*), 2.3 μm (*squares*), and 3.5 μm (*triangles*). Statistical uncertainties greater than 5% have been plotted, and the size of the typical overall uncertainty of 5% is shown in the lower right ×. Observations made in the same month have been averaged together.

FIG. 1.—The observed spectra of NGC 1068 ($z = 0.0036$), NGC 4151 ($z = 0.0033$), Mrk 231 ($z = 0.041$), and 3C 273 ($z = 0.158$), plotted at rest wavelengths. The spectrum of NGC 4151 was taken in 1977 December when the galaxy was near maximum brightness. The narrow-band and broad-band 10 μm data (*points, open circles,* and *open squares*), about which there might be some confusion, are all associated with Mrk 231 and not NGC 4151. The 3–4 μm portion of the 3C 273 spectrum has been smoothed by averaging together all points within 0.1 μm bins. The 1.6–2.3 μm portion of 3C 273 was taken from Puetter *et al.* (1978). *Squares,* broad-band observations from this work; ×, points taken from Rieke and Low (1972); *open triangles,* from Rieke and Low (1975); *open circles,* from Rieke (1976); the solid line in the 10 μm region of NGC 1068 is from Kleinmann, Gillett, and Wright (1976). The straight solid lines serve to connect various data sets.

TABLE 2

BROAD-BAND MAGNITUDES OF NGC 4151

Date (UT) (year/month/day)	1.65 μm	2.28 μm	3.5 μm
75/3/25	...	...	7.12
75/4/29	9.06	8.29	7.07
75/5/24	9.05	8.30	6.99
75/5/25	9.17	8.31	7.02
75/5/26	9.18	8.36	6.99
76/3/8	...	8.63	7.25
76/3/13	...	8.78	7.40
76/3/22	...	8.89	7.41
76/3/26	...	8.79	7.37
76/4/23	9.45	8.84	7.42 ± 0.12
76/4/24	9.48	8.83	7.55 ± 0.10
76/5/7	9.28	8.77	7.37
77/4/6	9.29	8.49	...
77/12/4[c]	9.15	8.27	...
77/12/5[c]	9.14	8.25	...
78/2/19	...	8.56	7.39
78/2/20	...	8.56	7.30
78/4/5[a]	...	...	7.34 ± 0.14
79/2/9	9.57	8.67	7.31
79/5/6	9.57	8.84	7.34
80/2/9[b]	9.04	8.30	7.02
80/2/10[b]	9.08	8.34	7.13
80/2/11[b]	9.09	8.23	7.02

[a] Observed with Si:As detector system.

[b] Measured linearly polarized component with E-vector in position angle 45°. Tabulated magnitudes assume that the source is unpolarized.

[c] The broad-band levels are discrepant with narrow-band fluxes on these nights. We believe that the spectrophotometric data represent the accurate level, so these magnitudes may be ∼25% too bright.

analysis of the spectrum of NGC 4151 is described below, and a representative spectrum of this galaxy, taken in 1977 December when the flux was near maximum, is shown in Figure 1. The 2 μm portion of the spectrum is similar to that of NGC 1068 and shows absorption from stellar H_2O and CO at 1.9 μm and 2.3 μm. The 3.1 μm H_2O feature was not seen because the signal-to-noise is relatively poor, and the stars contribute a smaller fraction of the flux, as discussed below. The spectrum of NGC 4151 in Figure 1 appears to show structure around 2.8 and 3.3 μm. The features shown are of low statistical significance, however, and were not confirmed by our other spectra. A more recent spectrum (Cutri and Rudy 1980) has shown a weak 3.3 μm emission feature.

III. DISCUSSION

a) NGC 1068

Penston *et al.* (1974) and Neugebauer *et al.* (1971) have measured the flux from NGC 1068 as a function of beam size at wavelengths from 0.5 μm to 3.4 μm. The measurements were interpreted as the sum of a spatially extended stellar component, which dominates the flux at 1.6 μm, and a point source, which dominates at 3.4 μm. In addition to the existence of a point source, the detection of neutral hydrogen and helium, and of molecular hydrogen (Thompson, Lebofsky, and Rieke 1978), indicates that the radiation arising from the nucleus of NGC

1068 cannot be attributed solely to stars. In our 17″ beam, however, the stellar component dominates the observed flux below 3 μm. Other measurements, using smaller beams (e.g., Thompson, Lebofsky, and Rieke 1978), contain relatively less stellar flux and thus have flatter slopes between 2.0 and 2.5 μm.

An attempt has been made to subtract out the stellar component from our spectrum in order to determine the energy distribution of the central source or sources. We assumed that the spectrum of the stellar component could be represented by a 3500 K blackbody with CO and H_2O absorption appropriate for late-type stellar atmospheres. Such an assumption is consistent with observations of the nuclear stellar population in another Sb galaxy, M31 (Sandage, Becklin, and Neugebauer 1969), which shows a spectral distribution in the near-infrared similar to that of M0 stars. In a first-order approximation, the stellar populations in the central regions of early spiral galaxies are similar to those in early elliptical galaxies. Therefore, an unpublished UCSD spectrum of M32, which has the same colors as a 3500 K blackbody in the 1–4 μm region (Penston *et al.* 1974) and a CO index of 0.15, according to the scale of Frogel *et al.* (1978), was assumed to be representative of the stellar flux from 2.1 to 2.5 μm. The depth of the H_2O absorption near 3.1 μm was taken to be the amount typical of M6 giants (Merrill and Stein 1976), one spectral subtype later than that indicated by the 1.9 μm H_2O absorption in most early-type galaxies (Aaronson, Frogel, and Persson 1978). This choice is intended to correct for the bias toward later stellar types, introduced by our observations which deal with an H_2O absorption at wavelengths of 2.8 to 3.5 μm, rather than 1.9 μm.

A suitable normalization of the stellar spectrum was found by using the multiaperture data of Penston *et al.* (1974) at 1.65 and 2.2 μm. Subtracting the smallest aperture measurements from those taken with a 15″ aperture gave the stellar flux from an annular region of ∼ 5″ to 15″ around the nucleus. This level was corrected to include the inner 5″ and to range out to 17″ (our beam size), by assuming that the flux follows a power-law dependence on beam diameter, $F \propto D^\gamma$, with $\gamma = 0.7$ at 1.65 μm and $\gamma = 0.45$ at 2.2 μm (Penston *et al.* 1974). The [1.6 μm] − [2.2 μm] color of this synthesized stellar component was in close agreement with that of M32. The [1.25 μm] − [1.65 μm] color of M32 then implies that the stars contribute no less than 95% of the total flux at 1.25 μm.

Figure 4 shows the assumed stellar spectrum normalized to 95% of the 1.25 μm flux and the resulting spectrum of the nucleus of NGC 1068. The level of the 10 μm data shown in Figure 1 remains unchanged because the stellar contribution declines steeply toward longer wavelengths. The lack of CO or H_2O features in the derived nuclear spectrum suggests that the level of the stellar spectrum has been chosen correctly. Also, the level is in agreement with the small aperture studies of Lebofsky, Rieke, and Kemp (1978).

The 8–13 μm spectrum of NGC 1068 is shown in Figure 2. This is generally similar to the spectrum published by
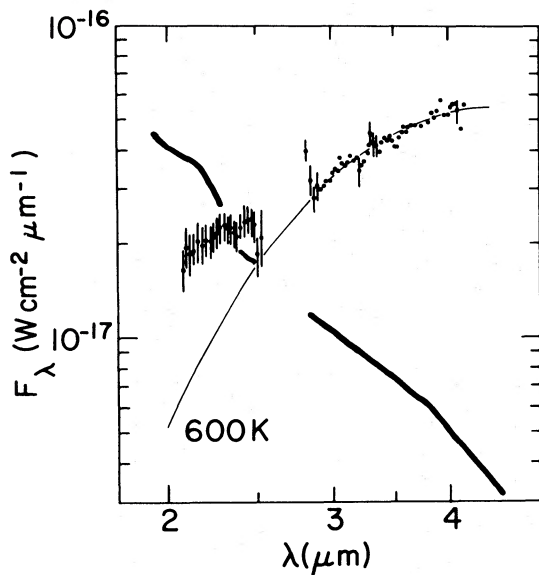
FIG. 4.—The deconvolution of the spectrum of NGC 1068. The heavy solid line represents the stellar component of the flux which has been assumed to comprise 95% of the 1.25 μm flux. The points are the nuclear spectrum, determined by subtracting the assumed stellar component from the observed spectrum. A 600 K blackbody curve is shown for comparison.

Kleinmann, Gillett, and Wright (1976) but of higher signal-to-noise. However, no flux in the 12.8 μm [Ne II] line was observed; the absence of emission was confirmed by further spectral scans (not shown) to a 3 σ limit of 4.5×10^{-19} W cm^{-2}. The 3 σ limits on other lines in the 8–13 μm region are [S IV] $< 1.0 \times 10^{-18}$ W cm^{-2} and [Ar III] $< 1.2 \times 10^{-18}$ W cm^{-2}. The nondetection of these lines is consistent with the observed Hβ flux, with an extinction $A_V \approx 1.2$ mag (Neugebauer et al. 1980), and with abundances from Allen (1973).

Fits to the spectrum were made of the form

$$F_\lambda(\text{calc}) = CF_\lambda(\text{em}) \exp\left(-\beta\tau_\lambda\right), \qquad (1)$$

where τ_λ is the normalized optical depth in the silicate absorption feature derived from the Trapezium region of Orion (Gillett et al. 1975), C is a normalizing constant, and $F_\lambda(\text{em})$ is the underlying emission. Three functions were used for $F_\lambda(\text{em})$: gray-body emission, $F_\lambda(\text{em}) = B_\lambda(T)$; optically thin silicate emission, $F_\lambda(\text{em}) = \tau_\lambda B_\lambda(T)$; and a power law, $F_\lambda(\text{em}) = (\lambda/10)^{\alpha-2}$. In the above equations, $B_\lambda(T)$ represents the Planck function nor-

malized to unity at 10 μm. The best-fit parameters and normalized χ^2 are shown in Table 3, where

$$\chi^2(\text{norm}) = \frac{1}{N_f} \sum_{i=1}^{n} \frac{[F_{\lambda,i}(\text{obs}) - F_{\lambda,i}(\text{calc})]^2}{\sigma_i^2}. \qquad (2)$$

The number of degrees of freedom $N_f = 38$. It can be seen from Figure 2 and Table 3 that the data may be acceptably fitted by either a power-law or gray-body emission, whereas optically thin silicate emission is ruled out. As noted by Kleinmann, Gillett, and Wright (1976), the smaller silicate-absorption optical depths ($0.4 \le \tau_{9.7} \le 0.6$) of these models are more nearly in agreement with estimates of visual extinction.

Although the power-law slope near 10 μm agrees with that found in the ultraviolet (Neugebauer et al. 1980), an extrapolation of the UV data to 10 μm results in a flux of only $\sim 3 \times 10^{-17}$ W cm^{-2} μm^{-1}, too low to account for the observed emission (Fig. 2). On the other hand, the requirement of gray-body emission can be achieved thermally in the following ways:

1. Optically thick silicate emission. To satisfy the required underlying flux at 10 μm, the emitting region must subtend only 0.5% of the surface area of the 1″ (110 pc) diameter nuclear source, and this restrains the emitting region to a distribution of condensations occupying 3×10^{-4} of the nuclear volume. The total infrared luminosity of the nucleus is $\sim 3 \times 10^{11}$ $L_\odot$ (Jones and Stein 1975), and if the condensations are heated by a single, central source of this luminosity, the grain temperature would be less than 90 K at a distance of 50 pc, compared with the observed color temperature of ~ 300 K. Alternatively, if each condensation is heated locally by its own source of luminosity, and if there are ~ 10 such condensations, silicate grains of typical size 0.05 μm would reach the observed temperature. In this model, the silicate extinction of $\tau_{9.7} \approx 0.5$ could be provided by a lower dust density distributed throughout the nuclear volume. The total silicate mass would be $\sim 7 \times 10^3$ $M_\odot$, if the mass absorption coefficient of silicates is 3.3×10^3 cm^2 g^{-1} (Gaustad 1963; Penman 1976).

2. In a medium containing a mixture of silicate grains and a small proportion by mass of infrared featureless grains, such as graphite, and heated by one or more sources of the required infrared luminosity, the graphite grains will reach a higher temperature than the silicate grains (Jones and Merrill 1976). Thus, the graphite grains could provide the observed emission and the colder silicate grains, the extinction (Kwan and Scoville 1976).

TABLE 3

MODEL FITS TO THE 8–13 μm SPECTRUM OF NGC 1068

Model	T(K)	β	C	$\alpha - 2$	χ^2/N_f
Optically Thick	301	0.63	9.08×10^{-17}	...	0.67
Optically Thin	301	2.21	4.05×10^{-16}	...	3.40
Power Law	...	0.43	7.60×10^{-17}	−0.20	0.78

There is no problem in accounting for the observed 20 μm silicate peak (Lebofsky, Rieke, and Kemp 1978) in either of these models, but only in the latter will the emission optical depth at 20 μm be related to the extinction depth at 10 μm.

The overall decline of the nuclear spectrum toward shorter wavelengths below 4 μm is clear, despite the uncertainty in the subtraction of the stellar flux. Neugebauer *et al.* (1980) found a $F_\nu \propto \nu^{-1.85}$ power-law flux component in the ultraviolet and suggested that, if it extends into the infrared, it may provide 50% of the 2.2 μm nuclear flux. Neither the level nor the slope of the nuclear infrared spectrum is dominated by such a component, and we conclude that it must cut off at shorter wavelengths. The nuclear spectrum can be represented by a steeper ($\nu^{-3.7}$) power law, between 2 and 4 μm. Such a flux distribution would be consistent with a nonthermal source of radiation only if its emission cuts off abruptly below 4 μm (cf. Rieke and Low 1975). Because such an abrupt cutoff is unlikely, and in light of the measurable angular size of the central source (Becklin *et al.* 1973) and the presence of silicate features at 10 and 20 μm, it is likely that the nuclear infrared radiation in NGC 1068 arises largely from thermal emission by dust. The decline in the spectrum from 4 to 3 μm probably represents the short wavelength cutoff of a thermal, spectral distribution from a dust shell. For comparison, Figure 4 shows the Wien end of a 600 K blackbody curve. Although uncertain, the spectrum may be broader than such a curve; there would then not be a sharp upper limit on the dust temperature (Panagia 1975).

If the dust is heated by a central source, the hottest temperature can be used to estimate the inner radius of the dust cloud. The infrared luminosity of the nuclear source in NGC 1068 is $\sim 3 \times 10^{11} L_\odot$ (Jones and Stein 1975), and gray grains would have to be closer to such a source than 1 pc in order to be as hot as 600 K. Nongray grains would be farther from the central source, and a distribution of temperature with radius could probably explain the size of $\sim 1''$ (Becklin *et al.* 1973) or 100 pc measured at 10 μm.

Although the nuclear spectrum is likely to be dominated by dust emission, analysis of the observed infrared polarization suggests that a nonthermal source is present as well (Lebofsky, Rieke, and Kemp 1978). The flux level adopted for such a source depends on its intrinsic polarization. For example, if the nonthermal source is intrinsically 10% polarized, it would contribute about 10^{-17} W cm^{-2} μm^{-1}, about one-fourth of the nuclear flux, at 3.5 μm (Fig. 4). The wavelength dependence of the polarized component depends on the reddening and intrinsic spectrum assumed, and the issue is complicated by apparent scattering at near-infrared wavelengths (Lebofsky, Rieke, and Kemp 1978). Nevertheless, it is likely that, at any wavelength between 1.5 and 5 μm, the flux from the nonthermal source is within a factor of 2 of that at 3.5 μm. Thus, while the nonthermal source may contribute a significant fraction of the nuclear flux shortward of 3 μm, most of the flux at longer wavelengths is probably due to thermal emission.

b) NGC 4151

The variability of NGC 4151 complicates an analysis similar to that employed for NGC 1068. As seen in Figure 2, maxima in 1.65 μm and 2.3 μm brightness occurred in 1975 April, 1980 February, and, nominally, in 1977 December, separated by minima in 1976 April and 1979 May. The variability at 3.5 μm is less clear. Variations of up to 35% between 1975 and 1976 seem to indicate some change; however, no appreciable variation was noted again until 1980. No periodicity is evident over the time scale of our observations.

In order to determine the energy distribution of the variable component of the spectrum, the observed fluxes at minimum brightness (1976 April) were subtracted from those at maximum brightness (1975 April). The difference can be approximated by a power law of the form $F_\nu \propto \nu^{-0.4}$. It must be noted, however, that minimum brightness does not occur coincidentally for all wavelengths. The nucleus is fainter at 1.65 μm in 1979 May than in 1976 April, for instance, but it is brighter at 3.5 μm. Consequently, the uncertainties in the value of the variable component's spectral index are high. Our initial value of the spectral index of $\alpha \sim 0.4$ is, however, consistent with the index derived from the variability of *UBV* measurements (Rieke 1978) and with the index of $\alpha \sim 0.33$ (Schmidt and Miller 1980), determined from the wavelength dependence of the optical polarization.

The agreement of the slope of the variable component we derive in the infrared with that derived in the optical suggests that the near-infrared variations may be due to the same source which produces the optical and UV variability. The required 1.65 μm brightness temperature is, however, only 750 K, based on a six-month time scale for significant variations (Penston *et al.* 1974, Fig. 3; Lebofsky and Rieke 1980), on a distance of 14 Mpc, and on the difference between minimum and maximum 1.65 μm fluxes. Thus the variable 1–3 μm emission might arise from dust heated by the nonthermal UV source, rather than from the nonthermal source itself. Existing variability data are insufficient to distinguish between these possibilities, but in this paper we will refer to the variable component as "the nonthermal component" because of its spectral energy distribution.

Optical observations suggest that the variations of the nonthermal source amount to nearly a factor of 2 (Penston *et al.* 1974). It is likely, therefore, that the energy distribution, at minimum, contains a nonthermal component roughly equal in flux to the difference between the maximum and minimum. We will assume that the spectral shape of the nonthermal component does not vary with time.

There is also evidence for a contribution by stars to the short wavelength flux. The variations at 1.65 μm are slightly smaller in magnitude than those at 2.3 μm. In addition, the aperture dependence measurements of the flux by Penston *et al.* (1974) show that there is a large contribution by spatially extended emission at the shorter wavelengths. Penston *et al.* (1974) have suggested that the stars in the nucleus of NGC 4151 also have colors similar to M32.

A minimum level for the stellar component was determined by a combination of methods. In the same manner as for NGC 1068, the multiaperture measurements of Penston *et al.* (1974) and Kemp *et al.* (1977) directly yield that the stars contribute nearly 99% of the 1.25 μm flux at minimum. Another estimate of the amount of stellar radiation can be found by assuming that the 1.25 μm light comes only from stars and the nonthermal source and that the variations in the nonthermal source amount to a factor of 2. Subtracting the difference between minimum and maximum from the flux at minimum thus yields a second estimate for the stellar component at 1.25 μm of 67% of the total. In order to set an upper limit on the nonstellar flux, an average value between the two, 81%, was adopted, and we consider it highly unlikely that the actual stellar contribution is smaller than this. For comparison, Rieke (1978) would find that the stars contribute more than 90% of the 1.25 μm flux. It was also assumed that the infrared colors of the stellar component are the same as those of M32, and in this manner, at minimum light, the stars were determined to contribute ~ 40% of the 2.3 μm flux, while the nonthermal source contributes ≤ 18%.

Subtracting the stellar and minimum nonthermal continua from the total spectrum at minimum reveals an infrared source that is dominant at longer wavelengths but decreases in flux below 3.5 μm. The deconvolution, shown in Figure 5, was first performed with the photometry of 1976 April, and the level of the resulting infrared component is represented by the open triangles. This component resembles the Wien end of a blackbody curve with a temperature of ~ 890 K. If this is taken to be the temperature of the inner edge of a dust cloud with an infrared luminosity of 10^{10} $L_\odot$ (Rieke 1978), an inner radius to the cloud of ~ 0.1 pc is implied. As seen in Figure 5, however, the nuclear infrared spectrum is broader than a single blackbody, and presumably a range of dust temperatures is required. Moreover, the actual geometry of the emitting region and the nature of the dust are uncertain, and the physical parameters given here are only estimates.

The spectral data of 1977 December, when the galaxy was slightly brighter, were also deconvolved. As seen in Figure 5, the shape of the infrared component, shown by the points, is consistent with that derived from the photometry at minimum light. The level is slightly higher, and a best-fit blackbody would be slightly hotter, as might be expected from a shell which is reradiating energy from a brighter central source. The presence of the stellar CO feature in the deconvolved spectrum verifies that the stellar flux is no lower and that the nonthermal source at minimum is no brighter than indicated in Figure 5.

An estimate, instead of an upper limit, for the flux density of the nonthermal source at minimum would have resulted from setting the stars to 94% of the 1.25 μm flux and decreasing the nonthermal source by a factor of 3. The longer-wavelength infrared component would be nearly unchanged. The decreased level of the nonthermal source is consistent with an extrapolation of the level of the variable ultraviolet component (Rieke 1978).

The data could also be explained in terms of a single nuclear spectral component in addition to the stars. The optical and infrared observations of Penston *et al.* (1974) show that a single power-law curve of index α ~ 1.1 could conceivably fit the nonstellar flux near maximum light. Because of the lack of simultaneous variations at all
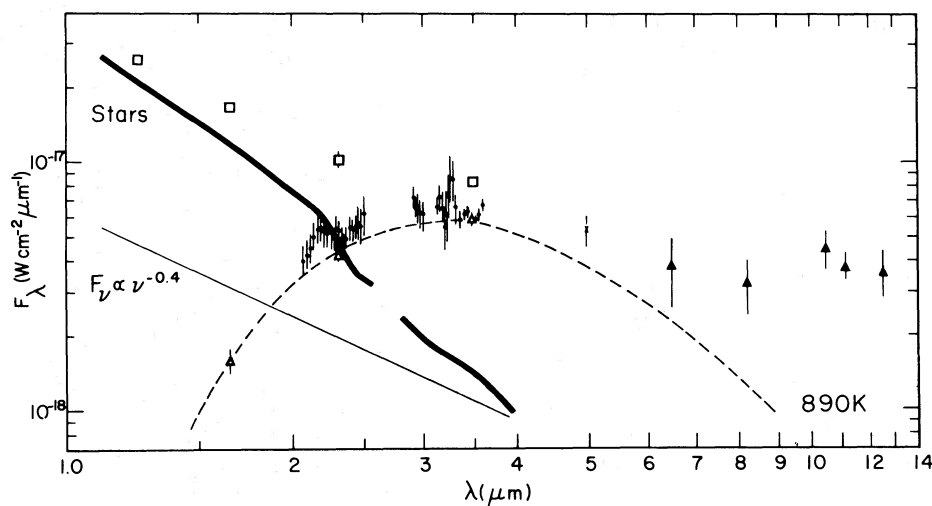

FIG. 5.—The deconvolution of the spectrum of NGC 4151 at minimum light. Open squares denote the broad-band measurements of 1977 April. The 5 μm broad-band × is from Rieke and Low (1972). The heavy solid line represents the stellar component of the flux, and the thin solid line represents the nonthermal component at minimum (see text). These two components subtracted from the broad-band points yield the spectrum of the infrared source (*open triangles*) fitted by an 890 K blackbody curve (*dashed line*). The small points are the resulting infrared component from the deconvolution of the spectral data of 1977 December. The filled triangles represent broad-band measurements; those beyond 8 μm were taken in 1977 April and May, and the 6.5 μm measurement was taken in 1978 May, from the Kuiper Airborne Observatory with a 27″ beam. These data are plotted without correction since there is little contribution by the stellar or nonthermal components at these wavelengths

optical and infrared wavelengths, however, such a component would need to vary in spectral shape, as well as in level. Additionally, at minimum light, several sharp spectral breaks must occur between 0.3 and 1 μm if the optical and infrared nonstellar radiation is to be attributed to a single source. The complexities of such a model lead us to postulate, instead, a model with three spectral components, all of which have constant spectral shape, and only one of which varies in level.

The three-component model could be fitted to each of our observations by choosing the level of the nonthermal source based on the shortest wavelength observed and on the assumed constant stellar flux. The predicted flux levels at longer wavelengths were then found to agree with the observations. However, the differences between the model and the observed flux levels averaged 0.12 mag and were correlated over a period of approximately 1 year. In 1975, 1977, and 1979, the model underestimates the longer-wavelength levels, while in 1976 and 1978, it predicts colors that are redder than those actually observed. This correlation, along with apparent phase differences between optical and infrared variations (Penston *et al.* 1974), may indicate that the slope of the nonthermal component changes with time. It could equivalently imply that the long-wavelength infrared source also varies but with a different time dependence from that of the nonthermal source. Such variation might be expected if the dust is significantly heated by the nonthermal source and if the dust cloud is extended. There is, however, firm evidence in the energy distribution and aperture dependence of the flux from NGC 4151 for the existence of at least three components: a stellar component which accounts for the spatially extended emission at 1.2–2.3 μm; a probably nonthermal component which accounts for the variability of the 1.6 and 2.3 μm flux levels; and a relatively constant infrared component, probably thermal in origin, which accounts for the bulk of the radiation at wavelengths longer than 3 μm. While a more complicated model may prove necessary, no model with fewer components will fit the data.

c) Markarian 231

The 2–4 μm portion of the spectrum of Mrk 231, shown in Figure 1, can be characterized by a single power-law curve of index $\alpha \sim 1.4$. In general, the level of the flux is consistent with that given by Rieke (1976), with the exception of the 1.25 and 1.65 μm broad-band points, which lie $\sim$ 30 and 15%, respectively, above Rieke's levels. The same points are 20 and 10% above those found by McAlary, McLaren, and Crabtree (1979); these discrepancies are discussed below. In light of the 5 μm measurement by Rieke (1976), it must be concluded that the spectrum flattens slightly toward longer wavelengths. No narrow structure is observed in the region of the 3.5 μm feature reported by Rieke (1976). However, the level of the 3.1–4.0 μm portion of our spectrum may be high, relative to a continuum defined by the 2 μm narrow-band data and the 5 μm point, and could lead to Rieke's (1976) conclusion of a 3.5 μm feature. In this case, an apparent feature in emission centered at a rest wavelength of $\sim$ 2.9 μm appears to be statistically significant. Conversely, if the narrow-band points between 3 and 4 μm are assumed to define the continuum, an apparent absorption feature may be seen at a rest wavelength of $\sim$ 2.8 μm. It is important to note, however, that these features are not present in all the spectra taken of Mrk 231. They are only significant in the 1977 December and 1979 March observations. While these features do appear to be statistically significant, their presence is dependent upon the level adopted for the continuum, and there is a possibility that they are the result of incomplete wavelength coverage as mentioned earlier. No good candidate for the identification of either feature is known.

The central source in Mrk 231 is significantly reddened by surrounding dust, possibly by up to 20 mag of visual extinction (Rieke 1976). Dereddening the observed fluxes by as much as this amount, or as little as 2 mag (Boksenberg *et al.* 1977), cannot produce an intrinsic spectral distribution that can be described by a single power-law curve between 1.2 and 22 μm. Rather, the spectrum apparently turns upward toward shorter wavelengths, reminiscent of a stellar spectrum (Rieke 1976). The discrepancy between the 1.25 and 1.65 μm flux densities reported by ourselves and by Rieke (1976) might be attributable to the fact that Rieke's measurements were made using beam sizes of 7$\overset{''}{.}$8 and 8$\overset{''}{.}$5, while ours were made with a 17$''$ beam. However, McAlary, McLaren, and Crabtree (1979) found only a 10% flux increase between 10$''$ and 15$''$ beams at wavelengths of 1.25 to 3.5 μm; their 15$''$ measurements at 1.25 and 1.65 μm are below our 17$''$ measurements. The dependence on aperture size of flux levels at 1.25 and 1.65 μm, if real, may also indicate a stellar component. If a stellar component is present and is a typical galactic population dominated by late-type stars, the absence from the spectrum of a 2.3 μm CO feature as deep as 5% suggests that stellar emission constitutes less than 25% of the total flux at 2.3 μm.

Boksenberg *et al.* (1977) have modeled the optical flux as either a reddened $\sim$ 10,000 K stellar blackbody or a reddened $F_\nu \sim$ constant spectrum. Even if either of these provides all of the 1.25 μm flux, they drop off too steeply to account for the longer-wavelength levels. Therefore, unless a $F_\nu \sim$ constant spectral component can provide the optical flux and then somehow slope significantly upward in the infrared, there must be a second component to the infrared flux which dominates at wavelengths longer than 2–3 μm. Joyce *et al.* (1975) show that problems with magnetic field strengths, particle lifetimes, and inverse Compton losses effectively rule out a synchrotron source for the infrared radiation in Mrk 231. Thermal dust emission is suggested by the apparent presence of silicates and the shape of the 5–22 μm energy distribution (Rieke 1976), by the wavelength dependence of polarization (Kemp *et al.* 1977), and by the evidence of dense gas clouds apparently being ejected from the nucleus (Adams and Weedman 1972). The data are, however, insufficient to determine whether there are two distinct spectral components or only a single component with a complicated energy distribution.

d) 3C 273

The absolute level of the spectrum of 3C 273 (shown in Fig. 1) agrees well with the levels reported by Rieke and Low (1972) and by Neugebauer *et al.* (1979). Slight discrepancies may be either calibration differences or small-scale ($< 10\%$) time variations, though no significant change has been noted since 1968 (Neugebauer *et al.* 1979). The overall spectrum can be roughly characterized by a power law with $F_\nu \propto \nu^{-1.0}$, representing a steepening from the optical (Neugebauer *et al.* 1979). More specifically, the continuum level remains essentially constant (in F_λ) between 1.6 and 2.5 μm, but slowly drops off past 2.5 μm, and thus is consistent with the 5 and 10 μm points of Rieke and Low (1972). One way to interpret this spectrum is as a power law with excess emission between 2 and 3 μm; alternatively, there could be a deficiency between 1.5 and 2.0 μm.

The most significant feature of the spectrum of 3C 273 is the presence of Pα at a rest wavelength of ~ 1.88 μm. On the basis of new optical observations, Puetter *et al.* (1981) conclude that the observed Pα/Hβ ratio and the Balmer decrement could be consistent with case B recombination line ratios, but intrinsic reddening is limited to $E_{B-V} \lesssim 0.1$. This result further supports the Grasdalen (1976) conclusion of minimal extinction of the central source, based on the Balmer decrement and the Pα/Hβ line ratio, and the same conclusion by Boksenberg *et al.* (1978), based on the lack of a broad 2200 Å dust absorption. If reddening is insignificant, then a single power-law curve, which may be sufficient to describe the optical data (Neugebauer *et al.* 1979), is insufficient to describe the infrared spectrum.

Neugebauer *et al.* (1979) have found that the spectral distribution of 3C 273 exhibits a flux excess in the 3 μm region. A similar but considerably smaller excess is evident in our spectrum; however, such a judgment is contingent on placement of the continuum. Recent theoretical calculations (Canfield and Puetter 1981, private communication) suggest that for optically thick models of QSO emission-line regions, there can be significant emission in the higher bound-free continua of hydrogen. The amount of flux predicted by these models might explain the observed emission bump in the 2–3 μm region.

Allen (1980) has reported an emission similar to the 3.27 μm features found in many objects showing dust emission, although his value for the continuum flux density is only about two-thirds of ours. Our spectral coverage is not sufficient to confirm this feature.

IV. CONCLUSIONS

The spectra of NGC 1068 and NGC 4151 can be explained only by a combination of components. Both galaxies show radiation from stars and from a component that decreases rapidly in flux to shorter wavelengths and is attributed to thermal dust emission. In addition, NGC 4151 shows a variable, probably nonthermal, component consistent with a power-law energy distribution. It is likely that a nonthermal component, which is necessary to explain the infrared polarization, is also present in the near-infrared flux of NGC 1068.

Mrk 231 shows no clear evidence for stellar emission from 2–4 μm, although stellar emission may be important at shorter wavelengths if there is significant reddening. No amount of reddening allows the intrinsic spectrum to be adequately approximated by a power law from 1.25 to 5 μm. The lack of CO absorption near 2.3 μm indicates that stars contribute less than one-fourth of the flux at this wavelength. Depending upon the placement of the continuum, either an emission feature at 2.9 μm or an absorption feature at 2.8 μm may have been detected. These features may, however, be spurious and should be reobserved.

The continuum spectrum of 3C 273 can be approximated by a power law from 1.2 to 10 μm, with some significant but small deviations. The observed fluxes fall below the power law near 1.5 μm (rest wavelength) and above, from 2 to 2.5 μm, for example. The discrepancies may be explainable if part of the continuum is a result of processes other than synchrotron emission.

REFERENCES

Aaronson, M., Frogel, J. A., and Persson, S. E. 1978, *Ap. J.*, **220**, 442.
Adams, T. F., and Weedman, D. W. 1972, *Ap. J. (Letters)*, **173**, L109.
Allen, C. W. 1973, *Astrophysical Quantities* (3d ed.; London: Athlone), p. 31.
Allen, D. A. 1976, *Ap. J.*, **207**, 367.
———. 1980, *Nature*, **284**, 323.
Angel, J. R. P., Stockman, H. S., Woolf, N. J., Beaver, E. A., and Martin, P. G. 1976, *Ap. J. (Letters)*, **206**, L5.
Becklin, E. E., Matthews, K., Neugebauer, G., and Wynn-Williams, C. G. 1973, *Ap. J. (Letters)*, **186**, L69.
Boksenberg, A., Carswell, R. F., Allen, D. A., Fosbury, R. A. E., Penston, M. V., and Savage, A. 1977, *M.N.R.A.S.*, **178**, 451.
Boksenberg, A., *et al.*, 1978, *Nature*, **275**, 404.
Burbidge, G. R., and Stein, W. A. 1970, *Ap. J.*, **160**, 573.
Canfield, R., and Puetter, R. C. 1981, *Ap. J.*, in press.
Cutri, R. M., and Rudy, R. J. 1980, *Ap. J. (Letters)*, **241**, L141.

Frogel, J. A., Persson, S. E., Aaronson, M., and Matthews, K. 1978, *Ap. J*, **220**, 75.
Gaustad, J. E. 1963, *Ap. J.*, **135**, 1050.
Gillett, F. C., Forrest, W. J., Merrill, K. M., Capps, R. W., and Soifer, B. T. 1975, *Ap. J.*, **200**, 609.
Grasdalen, G. L. 1976, *Ap. J. (Letters)*, **208**, L11.
Jones, T. W., Leung, C. M., Gould, R. J., and Stein, W. A. 1977, *Ap. J.*, **212**, 52.
Jones, T. W., and Merrill, K. M. 1976, *Ap. J.*, **209**, 509.
Jones, T. W., and Stein, W. A. 1975, *Ap. J.*, **197**, 297.
Joyce, R. R., Knacke, R. F., Simon, M., and Young, E. 1975, *Pub. A.S.P.*, **87**, 683.
Kemp, J. C., Rieke, G. H., Lebofsky, M. L., and Coyne, G. V. 1977, *Ap. J. (Letters)*, **215**, L107.
Kleinmann, D. E., Gillett, F. C., and Wright, E. L. 1976, *Ap. J.*, **208**, 42.
Kwan, J., and Scoville, N. Z. 1976, *Ap. J.*, **209**, 102.

Lebofsky, M. J., and Rieke, G. H. 1980, *Nature*, **284**, 410.
Lebofsky, M. J., Rieke, G. H., and Kemp, J. C. 1978, *Ap. J.*, **222**, 95.
McAlary, C. W., McLaren, R. A., and Crabtree, D. R. 1979, *Ap. J.*, **234**, 471.
Merrill, K. M., and Stein, W. A. 1976, *Pub. A.S.P.*, **88**, 285.
Neugebauer, G., *et al.* 1980, *Ap. J.*, **238**, 502.
Neugebauer, G., Garmire, G., Rieke, G. H., and Low, F. J. 1971, *Ap. J.* (*Letters*), **166**, L45.
Neugebauer, G., Oke, J. B., Becklin, E. E., and Matthews, K. 1979, *Ap. J.*, **230**, 79.
Pacholczyk, A. G., and Wisniewski, W. Z. 1967, *Ap. J.*, **147**, 394.
Panagia, N. 1975, *Astr. Ap.*, **42**, 139.
Penman, J. M. 1976, *M.N.R.A.S.*, **175**, 199.
Penston, M. V., Penston, M. J., Neugebauer, G., Tritton, K. P., Becklin, E. E., and Visvanathan, N. 1971, *M.N.R.A.S.*, **153**, 29.
Penston, M. V., Penston, M. J., Selmes, R. A., Becklin, E. E., and Neugebauer, G. 1974, *M.N.R.A.S.*, **169**, 357.

Puetter, R. C., Smith, H. E., Soifer, B. T., and Willner, S. P. 1978, *Ap. J.* (*Letters*), **226**, L53.
Puetter, R. C., Smith, H. E., Willner, S. P., and Pipher, J. L. 1981, *Ap. J.*, in press.
Rieke, G. H. 1976, *Ap. J.* (*Letters*), **210**, L5.
———. 1978, *Ap. J.*, **226**, 550.
Rieke, G. H., and Lebofsky, M. J. 1979, *Ann. Rev. Astr. Ap.*, **17**, 477.
Rieke, G. H., and Low, F. J. 1972, *Ap. J.* (*Letters*), **176**, L95.
———. 1975, *Ap. J.* (*Letters*), **199**, L13.
Sandage, A. R., Becklin, E. E., and Neugebauer, G. 1969, *Ap. J.*, **157**, 55.
Schmidt, G. D., and Miller, J. S. 1980, *Ap. J.*, **240**, 759.
Stein, W. A., Gillett, F. C., and Merrill, K. M. 1974, *Ap. J.*, **187**, 213.
Stein, W. A., and Weedman, D. W. 1976, *Ap. J.*, **205**, 44.
Thompson, R. I., Lebofsky, M. J., and Rieke, G. H. 1978, *Ap. J.* (*Letters*), **222**, L49.
Weedman, D. W. 1973, *Ap. J.*, **183**, 29.

D. K. AITKEN and P. F. ROCHE: Anglo-Australian Observatory, P.O. Box 296, Epping, NSW   2121, Australia

R. M. CUTRI: Steward Observatory, University of Arizona, Tucson, AZ   85721

B. JONES, R. C. PUETTER, R. J. RUDY, and S. P. WILLNER: Center for Astrophysics and Space Sciences C-011, University of California, San Diego, La Jolla, CA   92093

K. M. MERRILL: Kitt Peak National Observatory, P.O. Box 26732, Tucson, AZ   85726

R. W. RUSSELL: Astronomy Department, Cornell University, Ithaca, NY   14853

B. T. SOIFER: California Institute of Technology, 320–47, Pasadena, CA   91125